Cell, Vol. 77, 491–502, May 20, 1994, Copyright © 1994 by Cell Press

Disruption of the Mouse *mdr1a* P-Glycoprotein Gene Leads to a Deficiency in the Blood–Brain Barrier and to Increased Sensitivity to Drugs

A. H. Schinkel,* J. J. M. Smit,* O. van Tellingen,† J. H. Beijnen,‡ E. Wagenaar,* L. van Deemter,* C. A. A. M. Mol,* M. A. van der Valk,§ E.C. Robanus-Maandag,§ H. P. J. te Riele,§ A. J. M. Berns,§ and P. Borst*
*Division of Molecular Biology
†Department of Clinical Chemistry
§Division of Molecular Genetics
The Netherlands Cancer Institute
Plesmanlaan 121
1066 CX Amsterdam
The Netherlands
‡Slotervaart Hospital
Department of Pharmacy
Louwesweg 6
1066 EC Amsterdam
The Netherlands

Summary

We have generated mice homozygous for a disruption of the *mdr1a* (also called *mdr3*) gene, encoding a drug-transporting P-glycoprotein. The mice were viable and fertile and appeared phenotypically normal, but they displayed an increased sensitivity to the centrally neurotoxic pesticide ivermectin (100-fold) and to the carcinostatic drug vinblastine (3-fold). By comparison of *mdr1a* (+/+) and (−/−) mice, we found that the mdr1a P-glycoprotein is the major P-glycoprotein in the blood–brain barrier and that its absence results in elevated drug levels in many tissues (especially in brain) and in decreased drug elimination. Our findings explain some of the side effects in patients treated with a combination of carcinostatics and P-glycoprotein inhibitors and indicate that these inhibitors might be useful in selectively enhancing the access of a range of drugs to the brain.

Introduction

P-glycoproteins were initially identified through their ability to confer multidrug resistance (MDR) in mammalian tumor cells (Juliano and Ling, 1976). These large (140–170 kDa) plasma membrane proteins consist of two similar halves, each containing six putative transmembrane domains and an intracellular ATP binding site (Gros et al., 1986a; Chen et al., 1986). P-glycoproteins can confer multidrug resistance by actively extruding a wide range of structurally unrelated, amphiphilic hydrophobic drugs from the cell. Many of these drug substrates are toxic compounds of natural or semisynthetic origin (plants, fungi, bacteria), which are extensively used in the chemotherapy of cancer (e.g., Vinca alkaloids, anthracyclines, epipodophyllotoxins, actinomycin D, taxanes) or for a variety of other medical purposes such as immunosuppression (cyclosporin A, FK506). For reviews see Endicott and Ling (1989) and Gottesman and Pastan (1993).

Mammalian P-glycoproteins are encoded by small gene families, containing two members in humans (*MDR1* and *MDR3*) and three members in mice (*mdr1a*, *mdr1b*, and *mdr2*). *MDR1*, *mdr1a*, and *mdr1b* cDNAs can confer multidrug resistance, while the closely related *MDR3* and *mdr2* cDNAs apparently cannot (Gros et al., 1986b, 1988; Ueda et al., 1987; Hsu et al., 1989; Devault and Gros, 1990; van der Bliek et al., 1988; Schinkel et al., 1991; for alternative *mdr* nomenclatures, see Experimental Procedures). To learn more about the physiological role of P-glycoproteins, we have generated mice with a disruption of each of the P-glycoprotein genes. Using this approach, we have recently shown that the mouse mdr2 P-glycoprotein is indispensable for the secretion of phospholipids into bile (Smit et al., 1993). The function of the drug-transporting (mdr1-type) P-glycoproteins is less clear at the moment. The human MDR1 P-glycoprotein is present at high levels in the brush border of renal proximal tubules, at the biliary surface of hepatocytes, and at the apical surface of mucosal cells in small and large intestine (Thiebaut et al., 1987). In addition, *MDR1* is highly expressed in capillary endothelial cells of brain and testis (Cordon-Cardo et al., 1989; Thiebaut et al., 1989). Based on this tissue distribution, it has been proposed that MDR1 P-glycoprotein plays a role in the protection of the organism against toxic xenobiotics, by active excretion of these compounds into bile, urine, or intestinal lumen and by preventing accumulation in critical organs such as the brain. Human *MDR1* is also very highly expressed in the adrenal cortex and in placental trophoblasts. As the MDR1 P-glycoprotein is able to transport some natural steroid hormones, a physiological role of this protein in steroid secretion has been suggested (Sugawara et al., 1988; Ueda et al., 1992). The finding that MDR1 P-glycoprotein is associated with a volume-regulated chloride channel activity has led to the idea that it has a role in regulating epithelial cell volume (Valverde et al., 1992; Trezise et al., 1992).

In the mouse, these putative roles appear to be partially divided between the highly related *mdr1a* and *mdr1b* genes. The mdr1a and mdr1b P-glycoproteins have largely overlapping, but not identical drug transport capacities (Devault and Gros, 1990; Gros et al., 1991). Whereas *mdr1a* RNA is predominant in intestine, liver, brain, and testis, and *mdr1b* RNA is predominant in adrenal, placenta, ovarium, and uterus, both *mdr1a* and *mdr1b* RNA levels are substantial in the kidney. Heart, lung, thymus, and spleen also contain significant and similar levels of both *mdr1a* and *mdr1b* mRNA. In all major tissues, at least some RNA of both *mdr1a* and *mdr1b* was detectable by RNAase protection (Croop et al., 1989; Teeter et al., 1990; Arceci et al., 1988; our unpublished data).

Studies of P-glycoprotein (RNA) levels in clinical tumor samples indicate that this protein may be relevant for intrinsic or acquired multidrug resistance in a range of tumor

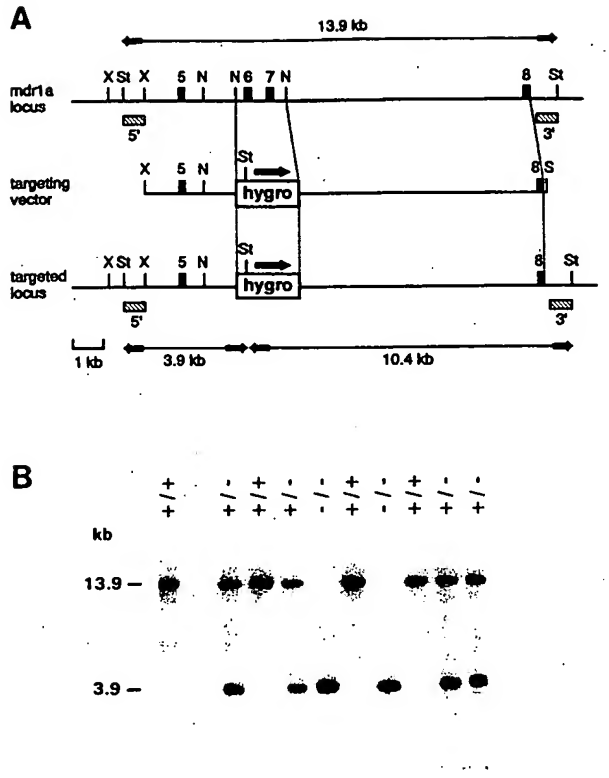

Figure 1. Targeted Disruption of the *mdr1a* Gene

(A) Structure of part of the *mdr1a* gene, the *mdr1a* targeting construct, and the predicted structure of the targeted *mdr1a* locus. Only relevant restriction sites are shown: N, NheI; S, SalI; St, StuI; X, XbaI. Numbered closed boxes represent exons. The large arrows indicate the direction of transcription of the *pgk–hygro* cassette (*hygro*). Hatched boxes indicate the position of the respective 5′ and 3′ probes used to detect homologous recombination. Two-headed arrows show the position and size of StuI restriction fragments diagnostic for proper targeting of the locus. Scale bar, 1 kb.

(B) Southern blot of StuI-digested genomic DNA of ten mice from one litter resulting from a cross between two *mdr1a* (+/−) mice. The blot was hybridized with the 5′ StuI–XbaI probe (see [A]). Fragment sizes and the *mdr1a* genotypes as derived from the hybridization pattern are indicated.

types (e.g., Goldstein et al., 1989; Chan et al., 1991), and this has led to a search for inhibitors. Many compounds with comparatively low cytotoxicity (such as verapamil, quinidine, cyclosporin A, and the nonimmunosuppressive cyclosporin D analogue PSC833) have been shown to inhibit P-glycoprotein activity (Tsuruo et al., 1981; Slater et al., 1986; for overview see Ford and Hait, 1990). There is currently an intense interest in the potential use of these so-called reversal agents in patients to reduce the P-glycoprotein-mediated resistance of clinical tumors. Several phase I and phase II trials towards this goal are already in progress (for a recent overview, see Sikic, 1993).

A major concern for this approach is the effect that efficient blocking of P-glycoprotein activity will have on the normal functioning of the organism. To obtain better insight into the pharmacological significance and into other possible biological roles of a drug-transporting P-glycoprotein, we have generated mice with a homozygous disruption of the *mdr1a* P-glycoprotein gene.

Results

Generation and Analysis of *mdr1a*-Deficient Mice

To disrupt the *mdr1a* gene, a 1.6 kb NheI genomic fragment containing exons 6 and 7 was replaced by a hygromycin phosphotransferase cassette in a targeting vector (see Figure 1A). This deletion removes the part of the gene encoding the putative transmembrane domains 2, 3, and 4, plus the first cytoplasmic and second extracellular loop of the protein. In addition, potential splicing over the selectable marker from exon 5 to exon 8 would result in a frameshift. The targeting construct was electroporated into E14 embryonic stem (ES) cells. Analysis of 71 hygromycin-resistant clones by Southern blotting indicated that 7 clones had undergone correct homologous recombination at both the 5′ and the 3′ junction and contained no additional integrations or recombinations of the targeting vector (data not shown).

Chimeric mice were generated by injection of independently isolated ES clones (29 and 313) into C57BL/6 blastocysts according to standard procedures (Bradley, 1987). Chimeric mice from each clone yielded germline transmission of the disrupted *mdr1a* allele. Heterozygotes (+/−) were viable and fertile and appeared to be normal. Separate interbreeding of heterozygotes derived from both clones readily yielded homozygous (−/−) mice. A representative Southern blot analysis of tail DNA from offspring of a cross between two (+/−) mice is shown in Figure 1B. Pooled data for crosses between clone 29 or clone 313 heterozygotes showed a distribution of 31% (+/+), 45% (+/−), and 24% (−/−) mice in 231 offspring analyzed. This suggests that disruption of the *mdr1a* gene does not affect viability of (+/−) or (−/−) mice at 4 weeks of age. Homozygous (−/−) mice, when interbred, are fertile and yield litters of comparable size as found in (+/+) interbreeding. The (+/−) or (−/−) mice could not be distinguished from the (+/+) mice by appearance or mortality rate up to 14 months of age. Analysis of the physiology, anatomy, and histology of (−/−) mice at various ages did not reveal clear abnormalities. Special attention was given to small and large intestine, where *mdr1a* expression is high, and to liver. In contrast with *mdr2* (−/−) mice (Smit et al., 1993), *mdr1a* (−/−) mice did not display abnormalities in biliary phospholipid or cholesterol levels, nor in bile acid output (R. P. J. Oude Elferink and A. K. Groen, personal communication). Levels of a range of serum enzymes, proteins, electrolytes, and other components as well as hematological parameters did not differ between *mdr1a* (+/+) and (−/−) mice (for details see Experimental Procedures).

mdr1a RNA and Protein in *mdr1a* (−/−) Mice

As the highest level of *mdr1a* RNA is found in intestinal tissue (Croop et al., 1989; Teeter et al., 1990; data not shown), we tested the effect of the gene disruption by RNAase protection on total RNA isolated from the small intestine. The *mdr1a* probe detects exons 17 and 18, approximately 1.5 kb downstream of exon 7 in the mRNA. Figure 2A shows that *mdr1a* RNA was considerably reduced, but still detectable in (−/−) mice. The very low level of intestinal *mdr1b* RNA was hardly affected by the disrup-

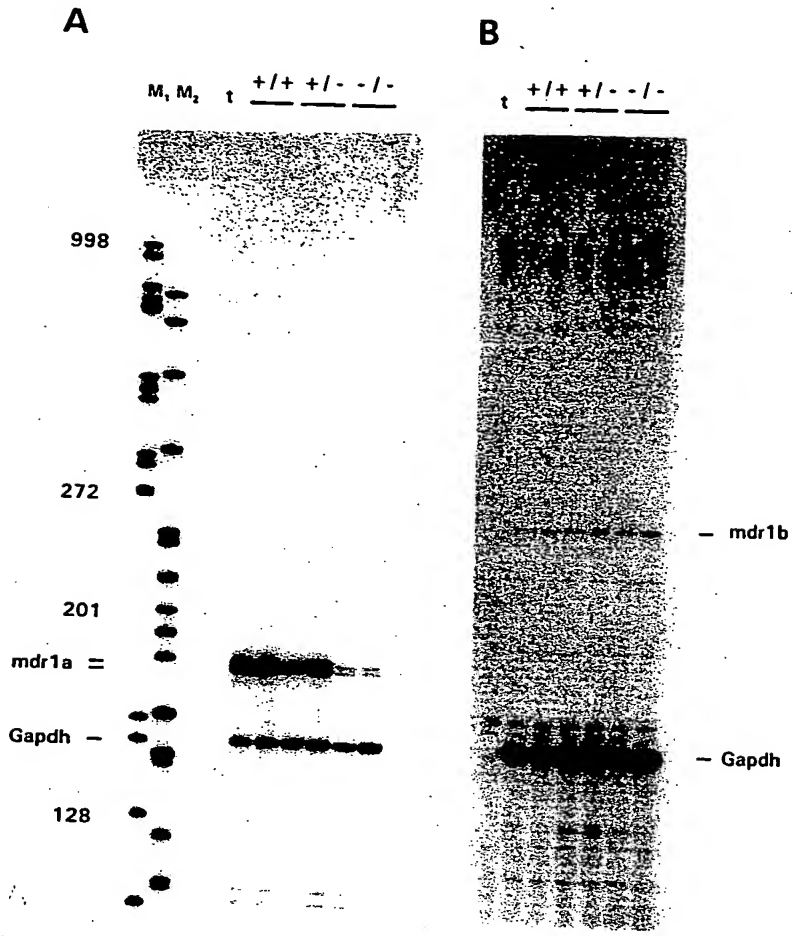

Figure 2. *mdr1a* and *mdr1b* RNA Levels in Small Intestine of *mdr1a* (+/+), (+/−), and (−/−) Mice

RNA levels were determined using RNAase protection on total RNA.

(A) *mdr1a* RNA levels. The positions of the *mdr1a*-protected (178 nt) and *Gapdh*-protected (150 nt) fragments are shown. The *mdr1a* genotype is indicated over each pair of lanes. For each genotype, one female (first lane) and one male (second lane) was analyzed. Lane t marks the transfer RNA control hybridization reaction. M1, end-labeled DdeI digest of M13 DNA. M2, end-labeled MspI-digest of pBR322 DNA. Some fragment sizes are indicated (see also Experimental Procedures).

(B) *mdr1b* RNA levels. The positions of the *mdr1b*-protected (255 nt) and *Gapdh*-protected (150 nt) fragments are shown. Specific activities of probes, order of samples, and other conditions were as in (A), but the gel in (B) was exposed much longer.

tion of the *mdr1a* gene (Figure 2B). As the low level of residual *mdr1a* RNA could originate in many different ways (readthrough of the *pgk* polyadenylation signal by transcripts initiated from the *mdr1a* promoter or from the *pgk* promoter, or transcription from cryptic promoters within the *mdr1a* gene downstream of exon 7; see also Smit et al., 1993), we tested whether this RNA could still encode detectable protein. For this purpose, we isolated epithelial cells from the villus region of duodenum, jejunum, and ileum of a (+/+) and a (−/−) mouse and analyzed the presence of P-glycoprotein on an immunoblot using the monoclonal antibody (MAb) C219. This antibody recognizes two conserved epitopes located in the first and second nucleotide-binding domains of both mdr1a and mdr1b P-glycoprotein, each encoded far downstream of the region deleted by the gene disruption (Georges et al., 1990). Figure 3 shows that no full-length P-glycoprotein was detectable in cells of the (−/−) mouse, nor could we detect shorter products different from the low molecular weight background bands equally visible in both (+/+) and (−/−) extracts. It thus appears unlikely that the residual *mdr1a* RNA gives rise to substantial amounts of protein. We therefore consider the *mdr1a* gene disruption to be a null mutation. A dilution series (data not shown) indicated that less than 2.5% of the wild-type mdr1a P-glycoprotein level would have been detectable, so we can further derive from this experiment that the mdr1b P-glycoprotein (to which C219 binds equally well) was absent, or present at only very low levels, in intestinal epithelial cells of *mdr1a* (−/−) mice.

Extreme Sensitivity of *mdr1a* (−/−) Mice to Ivermectin

By pure serendipity, we discovered that *mdr1a* (−/−) mice are extremely sensitive to ivermectin, an acaricide and anthelmintic drug. Shortly after we had obtained the first *mdr1a* (−/−) mice, all our mice were sprayed with a dilute solution of ivermectin to treat a mite infestation. This is generally a very safe procedure, even though the mice ingest part of the applied ivermectin by grooming of their coats. At this occasion, however, a number of mice died with paralytic symptoms, and subsequent tail DNA analysis showed that only *mdr1a* (−/−) mice had died, and no (+/+) or (+/−) mice. A systematic toxicity analysis demonstrated that *mdr1a* (−/−) mice are 50- to 100-fold more sensitive to orally administered ivermectin than genetically matched *mdr1a* (+/+) mice (Figure 4). *mdr1a* (−/−) mice derived from both clone 29 and 313 were hypersensitive, indicating that the observed effect was not due to a clonal idiosyncrasy. In spite of the vast difference in sensitivity, the highly characteristic symptoms of ivermectin toxicity in *mdr1a* (+/+) and (−/−) mice were comparable: immobilization, inability to right themselves, recumbency, tremors,

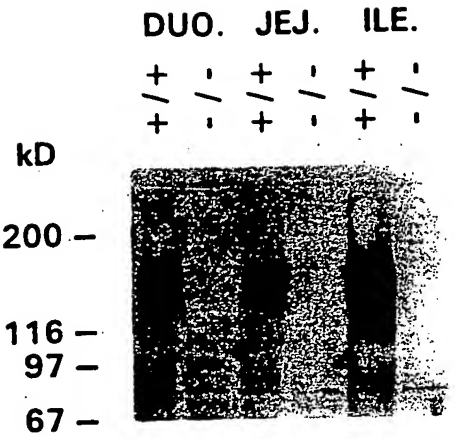

Figure 3. P-Glycoprotein Level in Intestinal Epithelial Cells of *mdr1a* (+/+) and (−/−) Mice

Protein immunoblot analysis of lysates from epithelial cells of the villus region of duodenum (duo.), jejunum (jej.), and ileum (ile.), using monoclonal antibody C219. The *mdr1a* genotype and the protein marker sizes are indicated. The amount and the intactness of total protein (10 μg) were identical in each pair of lanes as checked by staining with Ponceau S. The blot was deliberately overexposed to demonstrate the absence of P-glycoprotein in (−/−) lysates.

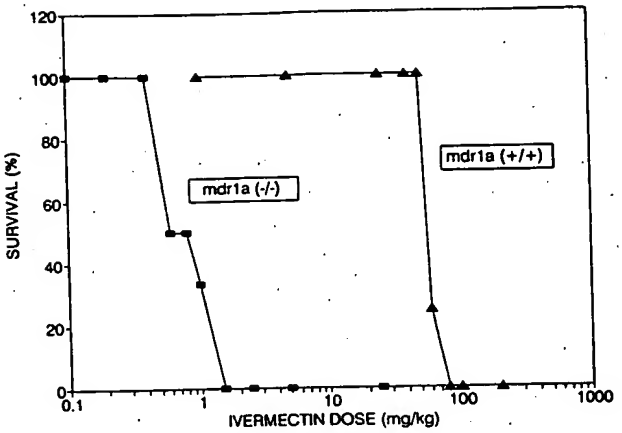

Figure 4. Ivermectin Toxicity in *mdr1a* (+/+) and (−/−) Mice

Toxicity was determined by checking survival during a 14-day period after oral administration of ivermectin to small groups (1–6 animals) of *mdr1a* (−/−) mice (rectangles), or *mdr1a* (+/+) mice (triangles). The numbers of mice tested at each dose were as follows: (−/−) mice, starting at 0.1 mg/kg: 2, 4, 4, 4, 4, 6, 4, 4, 2, 2. (+/+) mice, starting at 1 mg/kg: 2, 2, 4, 1, 6, 4, 4, 3, 2. Extrapolation from the graph yields an estimated LD_{50} of 0.7–0.8 mg/kg in (−/−) mice, and 50–60 mg/kg in (+/+) mice. (LD_{10} of 0.4–0.6 mg/kg and 40–60 mg/kg, respectively).

dramatically decreased breathing frequency, and finally onset of a comatose state that generally resulted in death.

Mdr1a P-Glycoprotein Functions in the Blood-Brain Barrier

The toxicity of ivermectin in mammals is thought to result from its interaction with a neurotransmitter system occurring only in the central nervous system. As the penetration of ivermectin into the brain of mammals is generally extremely low owing to the blood–brain barrier, ivermectin is very well tolerated by most mammals (for an overview, see Campbell, 1989). The blood–brain barrier is formed by the capillary endothelial cells of the brain, and P-glycoprotein is abundant in these cells in humans, rats, and hamsters (Cordon-Cardo et al., 1989; Thiebaut et al., 1989; Bradley et al., 1990). This protein might therefore contribute to the barrier by actively extruding drugs, such as ivermectin, from brain endothelial cells into the blood. Indeed, cultured mouse brain endothelial cell lines have been shown to transport vinblastine from basal (brain) to apical (blood lumenal) side in vitro (Tatsuta et al., 1992). If the *mdr1a* P-glycoprotein would be localized in the blood–brain barrier and capable of transporting ivermectin, this could explain the increased toxicity in *mdr1a* (−/−) mice. We therefore performed immunohistochemistry on brains of *mdr1a* (+/+) and (−/−) mice, using MAb C219. Figure 5 shows clear staining of capillaries in *mdr1a* (+/+) brain, and hardly any staining in *mdr1a* (−/−) brain. This indicates that the mdr1a P-glycoprotein is the predominant P-glycoprotein form present at the blood–brain barrier in wild-type mice and that little, if any, P-glycoprotein is present there in *mdr1a* (−/−) mice.

To test whether mdr1a P-glycoprotein can indeed exclude ivermectin from the brain, [^{3}H]ivermectin was administered orally to *mdr1a* (+/+) and (−/−) mice at a subtoxic dosage of 0.2 mg/kg, and tissue and plasma levels of radioactivity were determined 4 hr (data not shown) and 24 hr after dosing. Table 1 indicates that, after 24 hr, the level in the brain was indeed about 90-fold higher in (−/−) mice, whereas the levels in most tissues were only 3- to 4-fold higher than in (+/+) mice, roughly correlating with the 3-fold difference in plasma ivermectin level. The 3- to 4-fold overall increase could be due to increased net uptake of ivermectin from the gastrointestinal tract, to decreased elimination, or to both. Similar differences were found already 4 hr after dosing (data not shown). The 90-fold difference in brain concentration corresponds well with the 50- to 100-fold increased sensitivity of *mdr1a* (−/−) mice to ivermectin. The data indicate that mdr1a P-glycoprotein has a marked effect on the overall levels of ivermectin in the organism and a dramatic effect on concentration in the brain.

Mdr1a P-Glycoprotein Affects Vinblastine Distribution, Pharmacokinetics, and Toxicity

To study the role of mdr1a P-glycoprotein in the tissue distribution and excretion of a known substrate anticancer drug, we analyzed the levels of vinblastine in a range of tissues and compartments 4 hr after intravenous administration at a dosage of 1 mg/kg (Table 2) or 6 mg/kg (Table 3 and data not shown) in male (+/+) and (−/−) mice. Vinblastine was measured in tissue homogenates, using a sensitive and selective high-pressure liquid chromatography (HPLC) assay. Previous studies in mice indicate that at 4 hr, plasma vinblastine has reached equilibrium with most tissues, and further pharmacokinetics is dominated by elimination (van Tellingen et al., 1993a and 1993b). Table 2 demonstrates that, at a moderate dose, the absence of mdr1a P-glycoprotein had a clear effect on the vinblastine concentrations in heart, muscle, and brain,

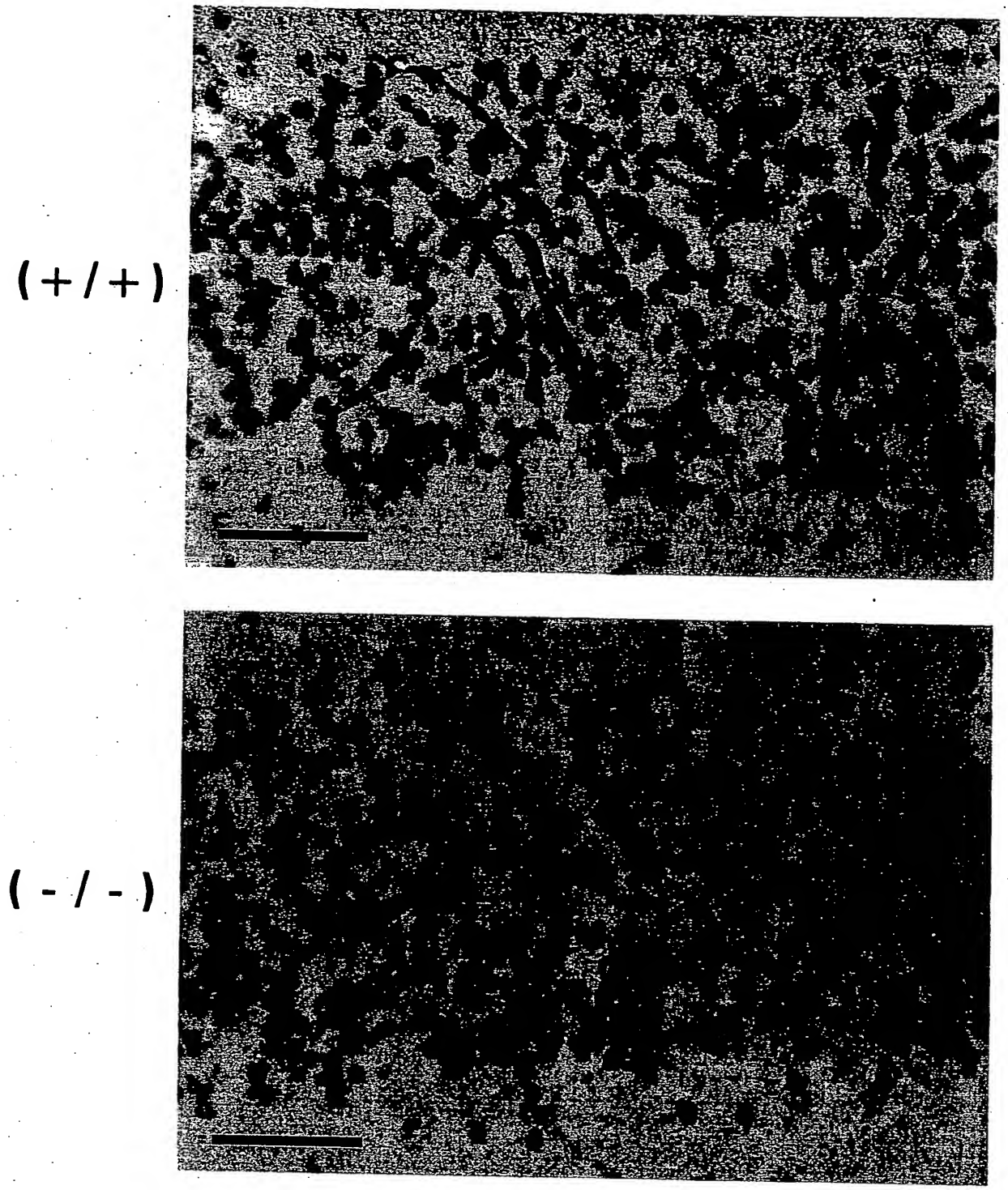

Figure 5. Presence of Mdr1a P-Glycoprotein in Capillary Blood Vessels of the Brain

Immunohistochemistry was performed on brain sections of *mdr1a* (+/+) and (−/−) mice using MAb C219, which detects all mouse P-glycoproteins. Red staining indicates binding of MAb C219 as visualized by a streptavidin-biotin peroxidase method. Light hematoxylin counterstaining was used. Comparable parts of the cerebellum are shown. Similar differences in staining of blood capillaries were observed throughout the cerebellum and cerebrum. Scale bar, 50 μm.

which were, respectively, about 3-, 7-, and 20-fold higher in *mdr1a* (−/−) mice, whereas the level in plasma was about 2-fold higher. Vinblastine concentrations in colon, small intestine, liver, kidney, lung, and testis were between 2- and 3-fold higher, and levels in other tissues ranged between 1- and 2-fold the levels in *mdr1a* (+/+) mice.

At 6 mg/kg, less pronounced differences were found between (+/+) and (−/−) mice, probably owing to satura-

Table 1. Tissue Concentrations of Ivermectin in *mdr1a* (+/+) and (−/−) Mice 24 hr after Oral Injection of a Dose of 0.2 mg/kg

Tissue	*mdr1a* (+/+)	*mdr1a* (−/−)	Ratio (−/−):(+/+)
Brain	1.5 ± 1.2	131 ± 16	87
Muscle	9.6 ± 3.3	48 ± 3	5.0
Heart	25 ± 10	100 ± 23	4.0
Kidney	47 ± 14	141 ± 27	3.0
Liver	130 ± 45	497 ± 74	3.8
Gall bladder	147 ± 17	1376 ± 804	9.4
Lung	23 ± 6	91 ± 24	4.0
Stomach	63 ± 60	107 ± 46	1.7
Small intestine	31 ± 13	121 ± 30	3.9
Colon	31 ± 12	108 ± 30	3.5
Fat (neck)	188 ± 62	486 ± 78	2.6
Fat (organ)	126 ± 77	152 ± 41	1.2
Testis	9.4 ± 4.2	70 ± 7	7.4
Epididymis	59 ± 20	164 ± 7	2.8
Spleen	13 ± 4	48 ± 10	3.7
Thymus	43 ± 13	121 ± 49	2.8
Plasma	16 ± 6	52 ± 8	3.3

Results are expressed as means ± SD (n − 1) in nanograms per gram of tissue. Three mice were analyzed in each group. All mice were male, between 10 and 14 weeks of age, and derived from ES cell clone 29.

Table 2. Tissue Concentrations of Vinblastine in *mdr1a* (+/+) and (−/−) Mice 4 hr after Intravenous Injection of a Dose of 1 mg/kg

Tissue	*mdr1a* (+/+)	*mdr1a* (−/−)	Ratio (−/−):(+/+)
Brain	5 ± 7	112 ± 18	22.4
Muscle	22 ± 9	148 ± 14	6.7
Heart	64 ± 15	219 ± 39	3.4
Kidney	399 ± 120	932 ± 75	2.3
Liver	115 ± 61	281 ± 75	2.4
Gall bladder	342 ± 143	466 ± 69	1.4
Lung	517 ± 47	1058 ± 191	2.1
Stomach	320 ± 96	563 ± 81	1.8
Small intestine	197 ± 25	577 ± 102	2.9
Coecum	467 ± 30	470 ± 94	1.0
Colon	214 ± 43	444 ± 51	2.1
Fat (neck)	213 ± 53	321 ± 35	1.5
Fat (organ)	88 ± 17	73 ± 1	0.8
Testis	26 ± 5	64 ± 3	2.5
Epididymis	233 ± 31	238 ± 23	1.0
Spleen	876 ± 111	1442 ± 89	1.7
Thymus	316 ± 16	426 ± 26	1.4
Lymph nodes	394 ± 68	496 ± 96	1.3
Plasma	3 ± 1	6 ± 1	2.0

Results are expressed as means ± SD (n − 1) in nanograms per gram of tissue. Three mice were analyzed in each group. All mice were male, between 10 and 14 weeks of age, and derived from ES cell clone 29.

tion of P-glycoprotein activity in many tissues (data not shown for all tissues). The level of vinblastine in plasma was the same in (+/+) and (−/−) mice, and the relative concentration ratios had dropped below 2 for most tissues. However, the vinblastine concentration in brain was still a striking 12-fold higher in *mdr1a* (−/−) mice (Table 3). Besides brain, only small intestine had a clearly higher (3-fold) vinblastine concentration in *mdr1a* (−/−) mice at this dosage (data not shown).

To assess the role of mdr1a P-glycoprotein in the elimination of vinblastine in the course of time, we also determined vinblastine concentrations in plasma, brain, heart, kidney, and liver at 4 hr, 8 hr, 24 hr, and 48 hr after intravenous injection of a 6 mg/kg dose in (+/+) and (−/−) mice. Table 3 shows that vinblastine was much more rapidly eliminated in (+/+) than in (−/−) mice, whereas the concentrations in all compartments (except brain) had been comparable at 4 hr. The most striking effect was observed in heart, which had a 7- to 14-fold higher concentration of vinblastine in *mdr1a* (−/−) mice between 8 hr and 24 hr after injection. The existing concentration difference in brain at 4 hr was further increased by the very slow elimination in (−/−) mice.

Together, these data indicate that the absence of mdr1a P-glycoprotein had a profound effect on the pharmacokinetics and tissue distribution of vinblastine, and by far the most striking effect was observed in brain. To examine the consequences of this marked difference in vinblastine handling, we carried out a limited vinblastine toxicity test in male *mdr1a* (+/+) and (−/−) mice (Table 4). The data indicate a 3- to 3.5-fold increase in sensitivity to intravenously administered vinblastine in *mdr1a* (−/−) mice. This increased sensitivity must be due to the increased access of vinblastine to tissues critical for vinblastine toxicity (possibly intestine) or to decreased elimination from these tissues. As the toxicity difference is lower than the brain

Table 3. Vinblastine Concentrations in Tissues and Plasma of *mdr1a* (+/+) and (−/−) Mice at Several Timepoints after Intravenous Injection of a Dose of 6 mg/kg

Tissue	Genotype	4 hr	8 hr	24 hr	48 hr
Brain	(+/+)	54 ± 9	47 ± 8	32 ± 4	9 ± 6
	(−/−)	663 ± 34	515 ± 68	734 ± 68	448 ± 14
Heart	(+/+)	1135 ± 342	76 ± 17	22 ± 9	0 ± 0
	(−/−)	1388 ± 80	540 ± 75	303 ± 48	25 ± 11
Kidney	(+/+)	6319 ± 1022	1605 ± 665	132 ± 31	22 ± 6
	(−/−)	5477 ± 516	3344 ± 890	1372 ± 711	60 ± 30
Liver	(+/+)	1588 ± 572	227 ± 162	34 ± 16	13 ± 13
	(−/−)	1966 ± 724	648 ± 140	192 ± 51	14 ± 11
Plasma	(+/+)	48 ± 10	10 ± 3	2 ± 1	0 ± 0
	(−/−)	43 ± 7	20 ± 2	10 ± 2	0 ± 0

Results are expressed as means ± SD (n − 1) in nanograms per gram of tissue. Three mice were analyzed from each group at each timepoint. All mice were male, between 10 and 14 weeks of age, and derived from ES cell clone 29.

Table 4. Vinblastine Toxicity in Male *mdr1a* (+/+) and (−/−) Mice

mdr1a (+/+)		*mdr1a* (−/−)	
Dose	Survival	Dose	Survival
8.8	100%	2	100%
13.2	100%	4	100%
17.6	83%	6	33%
22.0	67%	8	33%
28.6	17%	10	0%
35.2	0%		

The survival percentage at each vinblastine dose (in milligrams per kilogram, intravenous) is listed. For each dose, six animals were tested (five animals at 4 mg/kg). All mice were derived from ES cell clone 29.

concentration difference, brain toxicity is probably not a limiting factor for vinblastine, as it is for ivermectin. The macroscopic signs of toxicity in (+/+) and (−/−) mice were comparable: lethargy, immobilization, and refusal of food and water uptake.

Increased Expression of *mdr1b* in Kidney and Liver of *mdr1a* (−/−) Mice

Although the increased sensitivity to vinblastine and the increased penetration and decreased clearance of vinblastine in *mdr1a* (−/−) mice were clear, most vinblastine had still disappeared within 48 hr (see Table 3; data not shown). This probably is mainly achieved by metabolic modification and conjugation, followed by excretion (along other pathways than P-glycoprotein-mediated export) into bile, urine, and intestinal lumen (van Tellingen et al., 1993b). However, the mdr1b P-glycoprotein is also able to transport vinblastine (Gros et al., 1991), so this protein will probably contribute to the tissue distribution and excretion of this drug. We therefore checked by RNAase protection whether *mdr1b* RNA was affected by the disruption of the *mdr1a* gene in a range of tissues (see Experimental Procedures for tissues tested). Most tissues, including a number of tissues with significant *mdr1a* expression in wild-type mice (such as intestine and brain), did not have significantly altered levels of *mdr1b* expression in *mdr1a* (−/−) mice (Figure 2 and data not shown). However, in male *mdr1a* (−/−) or (+/−) mice, the expression of *mdr1b* in kidney was consistently and considerably increased relative to male (+/+) mice (Figure 6A). Note that wild-type females had a much higher *mdr1b* expression in kidney than wild-type males and that this also appeared to increase in (+/−) and (−/−) individuals. Protein immunoblot analysis confirmed these findings at the protein level (data not shown). A similar up-regulation of *mdr1b* expression was observed in the livers of male and female (+/−) and (−/−) mice (Figure 6B).

Since kidney and liver of *mdr1a* (+/−) mice show an intermediate increase in *mdr1b* expression, the observed overexpression either may be a compensatory response of the organ to the decrease of functional *mdr1a* or may be due to the genomic alteration in the *mdr1a* gene (insertion of the *pgk–hygro* cassette) directly affecting regulatory

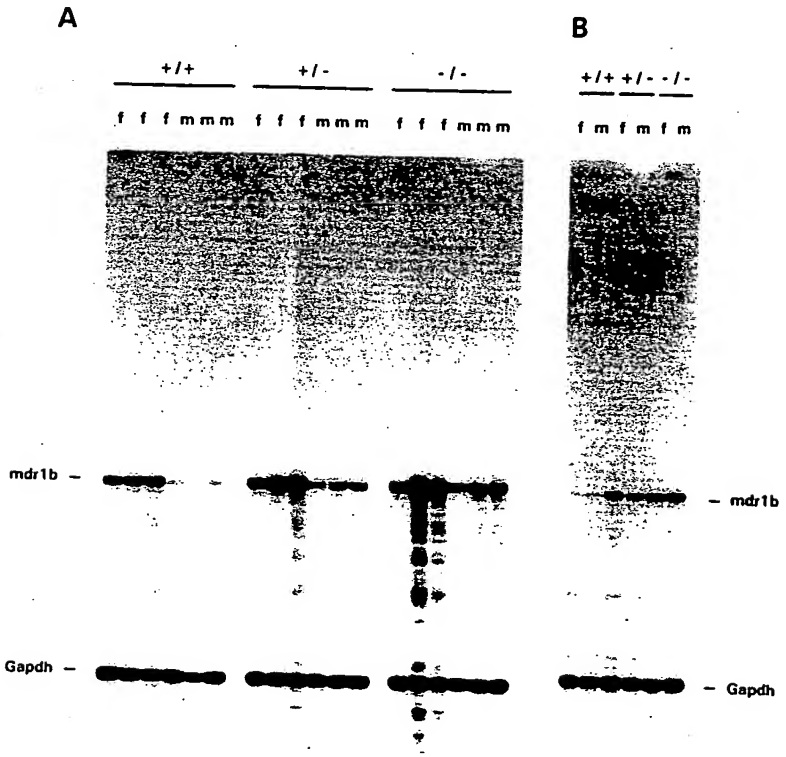

Figure 6. Levels of *mdr1b* RNA in Kidney and Liver of *mdr1a* (+/+), (+/−), and (−/−) Mice

RNA levels were determined by RNAase protection on total RNA from *mdr1a* (+/+), (+/−), and (−/−) mice.

(A) *mdr1b* RNA levels in kidney. For each genotype, RNAs from three females (f) and three males (m) were tested. The positions of the *mdr1b*-protected (255 nt) and *Gapdh*-protected (150 nt) fragments are indicated. The *mdr1a* genotypes are given over each set of lanes.

(B) *mdr1b* RNA levels in liver. Conditions and designations are as in (A).

elements of the *mdr1b* gene immediately downstream (Raymond et al., 1990). In view of the tissue specificity of the up-regulation in two pivotal excretory organs of the body, we favor the former possibility. This substantial increase in expression will probably compensate to some extent for the absence of functional mdr1a P-glycoprotein and, therefore, will limit the overall effects of the *mdr1a* knockout in drug handling and possibly in other processes.

Discussion

Our data show that the mouse mdr1a P-glycoprotein plays a major role in the defense of the organism against several xenotoxins of natural origin. This protective function will most likely extend to a whole range of plant, fungal, and bacterial toxins and carcinogens. In a natural situation, animals are confronted with a host of potentially harmful compounds in their diet, and they are therefore equipped with a battery of defensive mechanisms to avoid, exclude, remove, modify, or break down these products (Ames et al., 1990). The mdr1a P-glycoprotein appears to be an important element of this defense: removal of this single protein results in a 3- and 100-fold increased sensitivity to the two drugs tested, respectively.

The mdr1a P-glycoprotein appears to protect at at least two levels: first, it limits the amount of drug accumulating in certain tissues (brain, muscle, heart; Tables 1 and 2), and it speeds up the removal of drug from a tissue once plasma drug levels decrease (heart, kidney, liver; Table 3). Second, it enhances the rate at which drug is removed from plasma (Table 3), probably by stimulating excretion into bile and urine. The *mdr1a* expressed in intestine may also affect the net rate at which drug (ivermectin) is absorbed from the gastro-intestinal tract: the plasma ivermectin level was 3-fold lower in (+/+) than in (−/−) mice 4 hr after oral administration (data not shown; Table 1). However, this difference could also be caused by a higher elimination rate in (+/+) mice during this period, as is demonstrated by the plasma vinblastine levels 4 hr after intravenous administration of a 1 mg/kg dose (Table 2).

Increased plasma and tissue levels of vincristine and increased toxicity have been reported in mice receiving verapamil as a reversal agent (Horton et al., 1989). Our findings suggest that these effects were caused, at least in part, by blocking of mdr1-type P-glycoprotein activity, instead of other pharmacokinetic and pharmacodynamic interactions. In the *mdr1a* (−/−) mice, the endogenous *mdr1b* expression in many organs, combined with the increased *mdr1b* expression in kidney and liver, will limit the consequences of the *mdr1a* inactivation to a considerable extent: mdr1b P-glycoprotein transports vinblastine with about half the efficiency of mdr1a P-glycoprotein (Gros et al., 1991). We therefore expect that complete blocking of all mdr1-type P-glycoprotein activity will have even more severe consequences for the tissue distribution and pharmacokinetics of substrate drugs and, hence, for toxicity.

Implications for Efforts to Reverse Clinical MDR

Our findings have implications for the treatment of human cancer patients with cytostatic agents in combination with the more effective reversal agents currently developed or under study. Complete blocking of the single drug-transporting MDR1 P-glycoprotein in humans may result in drastic alterations of the pharmacokinetic parameters and tissue distribution of substrate drugs. Indeed, in clinical studies, increased plasma half-lives and toxicity effects have been observed for etoposide, daunorubicin, and doxorubicin when they were combined with the (partially) reversing agents verapamil or cyclosporin (for overview see Sikic, 1993). Major complications could arise when a certain drug is accumulated to a higher extent, or retained for a longer time, in a tissue that determines the critical toxicity of this drug. A case in point is the P-glycoprotein substrate doxorubicin, for which cardiotoxicity is dose limiting in humans. If doxorubicin would behave analogously to vinblastine, we would predict a strong increase in toxicity in human patients, owing to its increased accumulation and retention in heart (Tables 2 and 3). It is further obvious that the combined use of effective reversal agents and carcinostatic substrate drugs with significant central neurotoxicity should be avoided. The *mdr1a* (−/−) mice will be useful in identifying such neurotoxic drugs.

Unexpected hypersensitivity to other drugs, especially those with central nervous action, should also be anticipated. As illustrated by the ivermectin case, exposure to normally harmless compounds can result in disaster. Commonly used drugs such as morphine and digoxin are MDR1 P-glycoprotein substrates (Callaghan and Riordan, 1993; Tanigawara et al., 1992), but also the toxicity of the many other compounds known (or not yet known) to interact with P-glycoprotein could be affected (Ford and Hait, 1990; Gottesman and Pastan, 1993). We are currently investigating the effects of a range of cytostatic and noncytostatic drugs in the *mdr1a* (−/−) mice. The *mdr1a* knockout mouse model can also be used to test the in vivo efficiency of potential reversal agents, by comparing distribution and elimination of substrate drugs in normal mice treated with reversal agents and in *mdr1a* (−/−) mice receiving only the substrate drug.

Function of Mdr1a P-Glycoprotein in the Blood–Brain Barrier

The most pronounced pharmacological effect of mdr1a P-glycoprotein inactivation was seen in the brain, indicating that this protein plays an important role in the blood–brain barrier. Normally, the blood–brain barrier makes the brain a pharmacological sanctuary, rendering it barely accessible to a range of potentially useful drugs (Goldstein and Betz, 1986). Anatomically, the blood–brain barrier is located at the endothelial cells of the blood capillaries of the brain. Unlike endothelial cells elsewhere in the body, brain endothelial cells completely cover the walls of the capillaries, and they are linked to each other by tight junctions. Wide pores or fenestrations are absent in these cells. As a consequence, this cell layer acts as a continuous, lipophilic physical barrier, blocking the passive passage of hydrophilic solutes in either direction. The high metabolic needs of brain tissue are met by specific transport systems for glucose, amino acids, etc. across the endothelial cells. Relatively hydrophobic compounds such

as ethanol, caffeine, and nicotine can readily pass the blood–brain barrier, by passive diffusion through the membranes of the endothelial cells. In fact, most compounds obey the theoretically predicted linear relationship between brain endothelial permeability and the octanol/water partition coefficient ($\times MW^{-\frac{1}{2}}$), a measure of hydrophobicity (Bradbury, 1985). Interestingly, however, there are some striking exceptions to this rule, and these include the known P-glycoprotein substrates vincristine, doxorubicin, teniposide (VM-26), and cyclosporin A, each exhibiting a much lower endothelial permeability in rat brain than predicted (Levin, 1980; Cefalu and Pardridge, 1985; Saeki et al., 1993). Another notable exception is the dopamine antagonist domperidone (Laduron and Leysen, 1979). In view of the pronounced effect of the *mdr1a* inactivation on ivermectin and vinblastine accumulation in brain, it seems reasonable to attribute these discrepancies largely to P-glycoprotein action, as was previously suggested based on tissue distribution and functional studies (Cordon-Cardo et al., 1989; Thiebaut et al., 1989; Tatsuta et al., 1992). In theory, this opens the possibility to increase the brain penetration of a range of cytostatic P-glycoprotein substrate drugs by coadministration with effective reversal agents, possibly allowing better treatment of brain tumors (Greig et al., 1990). It may also be useful to increase the brain penetration of other noncytostatic drugs (such as antibiotics, antidepressants, or antipsychotics) that are P-glycoprotein substrates. Alternatively, it may even be possible to incorporate features of P-glycoprotein substrates into drugs to minimize their access to the brain or to promote brain entry by avoiding these features. The *mdr1a* (−/−) mice can be used as a model system to test the feasibility and consequences of such approaches.

Significance of P-Glycoprotein for the Use of Ivermectin

Before the *mdr1a* (−/−) mice died of ivermectin poisoning, we were not aware that this drug is a P-glycoprotein substrate. As ivermectin pharmacology is profoundly affected in *mdr1a* (−/−) mice, this drug appears to be a good substrate. Ivermectin is a slightly modified form of abamectin, a compound produced by the ground-dwelling bacterium Streptomyces avermitilis. Both compounds are widely used in tropical medicine, veterinary industry, and agriculture, owing to their efficiency as anthelmintic, acaricidal, and insecticidal agents, combined with a very high safety margin for toxicity in vertebrates (Campbell, 1989). Our data indicate that P-glycoprotein is a major determinant of this safety margin. Ivermectin is the drug of choice to treat river blindness (onchocerciasis), a blinding and debilitating disease caused by a parasitic nematode worm, which affects 18 million people in West Africa and Middle America (Taylor et al., 1990). Onchocerciasis patients are routinely treated with oral doses of 0.15 mg/kg of ivermectin. This is about two orders of magnitude below the lethal doses in a range of normal mammals, including mice, rats, dogs, rhesus monkeys, and probably also humans (Fisher and Mrozik, 1992). Yet, it is dangerously close to the lethal dose in *mdr1a* (−/−) mice (0.6 mg/kg; see Figure 4).

Extreme ivermectin sensitivity has been reported in some inbred dogs of the collie breed. The lethal oral dose was approximately 0.4 mg/kg, as opposed to approximately 80 mg/kg in normal dogs. Hypersensitivity was associated with highly increased ivermectin accumulation in the brain (Pulliam et al., 1985). Based on this strong analogy with the *mdr1a* (−/−) mice, we expect these dogs to have a similar genetic deficiency in an mdr1-type P-glycoprotein. It is interesting to note that more than 10 million people have been treated with ivermectin (0.15 mg/kg) without indications for a similar hypersensitivity. This may indicate that a genetic deficiency in the single MDR1.P-glycoprotein gene of humans is not compatible with life, but it is also possible that the symptoms of hypersensitivity have been misinterpreted.

Does Mdr1a P-Glycoprotein Have Other Functions?

Apart from the protective role of mdr1a P-glycoprotein, we have found no indications for additional functions of this protein. This may mean that there is no other function, that such a function does not become apparent under laboratory conditions, or that such a function is taken over by another protein. An obvious candidate is the highly related mdr1b P-glycoprotein, which is expressed in many tissues and even overexpressed in kidney and liver of *mdr1a* (−/−) mice. The only way to definitively answer this question is to generate mice with a disruption of both the *mdr1a* and *mdr1b* genes. In view of the very close linkage of these two genes (Raymond et al., 1990), this cannot be done by crossing mice deficient in either gene. Therefore, we are currently trying to generate these mice by disrupting both the *mdr1a* and *mdr1b* genes on the same chromosome in ES cells.

Experimental Procedures

P-Glycoprotein Nomenclature

The mouse *mdr1a* gene is also called *mdr3* (Hsu et al., 1989; Devault and Gros, 1990). The mouse *mdr1b* gene is also called *mdr1* (Gros et al., 1988; Hsu et al., 1989). The human *MDR3* gene is also called *MDR2* (van der Bliek et al., 1988; Roninson et al., 1986).

Construction of the Targeting Vector

Molecular–biological techniques were carried out according to standard procedures (Sambrook et al., 1989). *mdr1a* genomic sequences were isolated from an EMBL-3 λ phage library constructed with DNA from a mouse strain 129-derived CCE ES cell line. *mdr1a* sequences were identified by restriction mapping and partial sequencing of exons. This showed that the exon composition of *mdr1a* in the 5′ genomic region is collinear with that of *mdr1b* (data not shown; Raymond and Gros, 1989). The backbone for the targeting construct was a 12.5 kb genomic *mdr1a* fragment stretching from a genomic XbaI site approximately 1 kb upstream of exon 5 to a SalI site in the EMBL-3 polylinker attached to a genomic MboI site just downstream of exon 8 (see also Figure 1A). This fragment was cloned in pGEM-3Zf(−) (Promega). The 1.6 kb NheI fragment containing exons 6 and 7 was removed by partial digestion with NheI and replaced by a 2 kb XbaI fragment containing a *pgk–hygro* cassette: the bacterial *hygro* gene under the control of a mouse *pgk* promoter and polyadenylation signal (Kaster et al., 1983; van der Lugt et al., 1991; see also Smit et al., 1993). The targeting construct was released from the vector by digestion with XbaI and SalI, yielding a 5′ end with complete homology to the *mdr1a* gene and a 3′ end containing a short section of the EMBL-3 polylinker.

Electroporation and DNA Analysis of ES Cells (and Mice)

Electroporation and selection of 129/Ola-derived E14 ES cells were as described (Smit et al., 1993), except that hygromycin B (Calbiochem)

selection (at 150 μg/ml) was used. Homologous recombination in ES clones was checked by DNA blotting: after digestion of genomic DNA with StuI, size separation in a 0.8% (w/v) agarose gel, and transfer to nitrocellulose filter, the 5′ junction was checked by hybridization with a 0.5 kb StuI–XbaI probe positioned immediately 5′ of the targeting construct, and the 3′ junction was checked with a 0.6 kb BglII–StuI fragment positioned immediately 3′ of the targeting construct (see Figure 1A). Absence of additional random integrations of the targeting construct was checked by hybridization with a *hygro* probe. Tail DNA blot analysis of *mdr1a* (−/−) mice with a probe covering exons 6 and 7 confirmed that the genomic region containing exons 6 and 7 of *mdr1a* was completely absent from genomic DNA.

RNA Analysis

Isolation of total RNA from mouse tissues and RNAase protection assays were as described (Smit et al., 1993). RNAase protection constructs, transcription, and length of protected fragments were as follows.

mdr1a

An ApaI–StyI (blunted) *mdr1a* cDNA fragment (position 1615–2274 relative to the translation start) was cloned in an ApaI–ClaI (blunted) pGEM-7 vector. After linearization with EcoRI (position 2096), transcription with SP6 RNA polymerase generated a 234 nt probe, yielding a protected *mdr1a* fragment of approximately 178 nt, overlapping exons 17 and 18.

mdr1b

A BamHI–BstYI *mdr1b* cDNA fragment (position 2091–2339 relative to the translation start) was cloned into BamHI-digested pGEM-11. After linearization with BamHI (position 2091), a 291 nt probe was generated by transcription with SP6 RNA polymerase, yielding a protected *mdr1b* fragment of approximately 255 nt, overlapping exons 17, 18, and 19.

gapdh

A 149 nt BstEII (blunted)–HindIII *gapdh* cDNA fragment (position 92–240 in the cDNA sequence, accession code M32599) was subcloned in HincII–HindIII digested pGEM-3. After linearization with XbaI, transcription with SP6 RNA polymerase generated a 163 nt probe, yielding a 150 nt *gapdh*-protected fragment.

Size markers were an end-labeled DdeI digest of M13 DNA, yielding fragments (>100 nt) of 998, 865, 652, 600, 575, 563, 399, 381, 367, 303, 294, 272, 160, 153, 128, and 109 nt; and an end-labeled MspI digest of pBR322 DNA, yielding fragments (>100 nt) of 622, 527, 404, 309, 242, 238, 217, 201, 190, 180, 160, 147, 122, and 110 nt. The following tissues of male and female *mdr1a* (+/+), (+/−), and (−/−) mice were tested for both *mdr1a* and *mdr1b* expression: brain, heart, lung, muscle, liver, kidney, adrenal, stomach, duodenum, jejunum, ileum, coecum, colon, spleen, thymus, testis, ovarium, and uterus.

Maintenance and Analysis of Mice

Animals were kept as described (Smit et al., 1993). All experiments with *mdr1a* (−/−), (+/−), and (+/+) mice were carried out in a mixed genetic background (effectively F2 and F3 generations of a cross between 129/Ola and FVB mice). Most experiments were done with mice derived from clone 29, but phenotypic abnormalities, such as ivermectin hypersensitivity, were also checked in mice derived from clone 313. Serum or blood samples from mice were taken by orbital bleeding or heart punction. Serum levels of bilirubin, alkaline phosphatase, aspartate aminotransferase, alanine aminotransferase, lactate dehydrogenase, 5′-nucleotidase, creatinine, urea, Na^+, K^+, Ca^{2+}, inorganic phosphate, Cl^-, total protein, and albumin were determined on a Hitachi 911 analyzer according to the instructions of the manufacturer. Hemoglobin level, the hematocrit, and erythrocyte, leucocyte, and thrombocyte counts were determined on a Coulter model T660 cell counter. Collection and analysis of bile, and mouse tail DNA isolation were performed as previously described (Smit et al., 1993).

Immunohistological, Histological, and Anatomical Analyses

Mice were examined macroscopically before and during dissection. Light microscopy of tissues was as described (Smit et al., 1993). Intestinal samples were subjected to morphometric analysis of the intestinal wall. For immunohistochemistry, frozen brains were sectioned at 5 μm thickness, air dried, and fixed in acetone for 10 min at room temperature. Subsequent incubations and rinses were also performed at room temperature. After preincubation with 10% normal rabbit serum, sections were incubated for 60 min with MAb C219 (16 μg/ml). A streptavidin–ABC horseradish peroxidase procedure (DAKO, Glostrup, Denmark) was used for detection of the primary antibody: after two rinses in phosphate-buffered saline, slides were incubated with biotinylated rabbit anti-mouse IgG antibody (diluted 1:1000) for 30 min, followed by three rinses with phosphate-buffered saline, after which slides were incubated with the streptavidin-biotin peroxidase complex for 30 min, rinsed, and incubated for 10–15 min in a 3-amino-9-ethylcarbazole solution. A light hematoxylin counterstain was used. As a control for background staining, parallel incubations were performed without primary antibody.

Protein Analysis

Protein immunoblot analysis of P-glycoprotein content of cell or tissue lysates was carried out as described (Schinkel et al., 1991), except that MAb C219 binding was visualized using the enhanced chemiluminescence procedure (Amersham). Intestinal epithelial cells mainly derived from the villus region were isolated as described (van Dommelen et al., 1986). Protein concentration was determined with a Bio-Rad protein assay, using bovine serum albumin as a standard.

Toxicity and Drug Distribution Experiments

Unless indicated otherwise, all toxicity and drug distribution experiments were carried out with male mice between 9 and 14 weeks of age. In acute toxicity experiments, mice were observed for a period of 2 weeks.

Ivermectin Toxicity

A concentrated ivermectin stock (100 mg/ml) was obtained by lyophilization of a commercially available injectable formulation containing 10 mg/ml ivermectin ("Ivomec," Merck, Sharp, and Dohme AgVet). Suitable dilutions of this stock were made in 1,2-propanediol. For oral administration, proper doses were prepared in 70% (v/v) sesame oil, 30% (v/v) 1,2-propanediol at concentrations allowing dosing at a ratio of 10 μl per gram of mouse. On average, 250 μl to 350 μl of thoroughly mixed suspension was administered directly into the stomach by injection with a blunt-ended, bent needle inserted via the mouth and oesophagus. Lethal toxicity occurred between a few hours and maximally 6 days after injection.

Vinblastine Toxicity

Vinblastine sulphate (Lederle Nederland BV, Etten-Leur, or Medgenix Group) was dissolved, diluted, and administered in sterile 5% (w/v) D-glucose solution. Concentrations were adjusted to allow injection of 5 μl per gram body weight. On average, between 125 μl and 175 μl was injected with a 23 gauge injection needle in the tail vein of mice lightly anesthetized with diethyl ether (injection time: 5 s). Lethal toxicity occurred between 3 and 7 days after injection.

Vinblastine Distribution

Vinblastine sulphate was injected in the tail vein of mice as described above. Determination of the vinblastine concentrations in plasma and a range of tissues was carried out using a sensitive and highly specific analytical procedure based on high performance liquid chromatography and fluorescence detection as described before (van Tellingen et al., 1993b).

Ivermectin Distribution

[22,23-^{3}H]ivermectin B1a (specific activity 51.9 mCi/mg) was diluted with carrier ivermectin (both compounds provided by Dr. J. Schaeffer, Merck Research Laboratories) and formulated in 2% (v/v) 1,2-propanediol, 98% (v/v) sesame oil to a final specific activity of 0.333 mCi/mg. This ivermectin solution was orally dosed into the stomach as described above, at a dose of 0.2 mg/kg. On average, between 2 μCi and 2.5 μCi was injected per mouse. Tissues were collected at specific time points, weighed, and homogenized in 4% (w/v) bovine serum albumin solution. A 200 μl aliquot was transferred to Ultima gold counting fluid (Packard), and radioactivity was determined by liquid scintillation counting.

Acknowledgments

We thank D. M. Majoor and Dr. W. J. Mooi for the immunohistochemistry; J. Jonkman and Dr. W. J. Nooijen for the serum clinical chemistry analyses; A. J. Schrauwers, N. Bosnie, and A. Zwerver for excellent biotechnical assistance; Dr. M. A. van Roon and N. M. T. van der Lugt

for blastocyst injections; and Drs. G. Rudenko, G. J. R. Zaman, and R. H. A. Plasterk, and A. J. Smith and E. W. H. M. Eijdems for advice and support throughout the course of this work and critical reading of the manuscript. We also thank Drs. P. Gros and J. K. Heath for providing cDNAs; Dr. G. Grosveld for the mouse genomic library; Dr. M. Hooper for E14 ES cells; Drs. J. M. Schaeffer and L. H. T. van der Ploeg for providing labeled ivermectin; Dr. H. R. de Jonge for preparation of intestinal epithelial cells; and Drs. A. K. Groen and R. P. J. Oude Elferink for communicating unpublished results. This work was supported in part by grants NKI 88-6 and NKI 92-41 of the Dutch Cancer Society to P. B.

Received February 11, 1994; revised March 18, 1994.

References

Ames, B. N., Profet, M., and Gold, L. S. (1990). Nature's chemicals and synthetic chemicals: comparative toxicology. Proc. Natl. Acad. Sci. USA *87*, 7782–7786.

Arceci, R. J., Croop, J. M., Horwitz, S. B., and Housman, D. (1988). The gene encoding multidrug resistance is induced and expressed at high levels during pregnancy in the secretory epithelium of the uterus. Proc. Natl. Acad. Sci. USA *85*, 4350–4354.

Bradley, A. (1987). Production and analysis of chimeric mice. In Teratocarcinomas and Embryonic Stem Cells: A Practical Approach, E. J. Robertson, ed. (Oxford: IRL Press), pp. 113–152.

Bradley, G., Georges, E., and Ling, V. (1990). Sex-dependent and independent expression of the P-glycoprotein isoforms in Chinese hamster. J. Cell. Physiol. *145*, 398–408.

Bradbury, W. B. (1985). The blood–brain barrier: transport across the cerebral endothelium. Circ. Res. *57*, 213–222.

Callaghan, R., and Riordan, J. R. (1993). Synthetic and natural opiates interact with P-glycoprotein in multidrug-resistant cells. J. Biol. Chem. *268*, 16059–16064.

Campbell, W. C. (1989). Ivermectin and Abamectin. (New York: Springer-Verlag).

Cefalu, W. T., and Pardridge, W. M. (1985). Restrictive transport of a lipid-soluble peptide (cyclosporin) through the blood–brain barrier. J. Neurochem. *45*, 1954–1956.

Chan, H. S. L., Haddad, G., Thorner, P. S., DeBoer, G., Lin, Y. P., Ondrusek, N., Yeger, H., and Ling, V. (1991). P-glycoprotein expression as a predictor of the outcome of therapy for neuroblastoma. N. Engl. J. Med. *325*, 1608–1614.

Chen, C., Chin, J. E., Ueda, K., Clark, D. P., Pastan, I., Gottesman, M. M., and Roninson, I. B. (1986). Internal duplication and homology with bacterial transport proteins in the *mdr1* (P-glycoprotein) gene from multidrug-resistant human cells. Cell *47*, 381–389.

Cordon-Cardo, C., O'Brien, J. P., Casals, D., Rittman-Grauer, L., Biedler, J. L., Melamed, M. R., and Bertino, J. R. (1989). Multidrug-resistance gene (P-glycoprotein) is expressed by endothelial cells at blood–brain barrier sites. Proc. Natl. Acad. Sci. USA *86*, 695–698.

Croop, J. M., Raymond, M., Haber, D., Devault, A., Arceci, R. J., Gros, P., and Housman, D. E. (1989). The three mouse multidrug resistance (*mdr*) genes are expressed in a tissue-specific manner in normal mouse tissue. Mol. Cell. Biol. *9*, 1346–1350.

Devault, A., and Gros, P. (1990). Two members of the mouse *mdr* gene family confer multidrug resistance with overlapping but distinct drug specificities. Mol. Cell. Biol. *10*, 1652–1663.

Endicott, J. A., and Ling, V. (1989) The biochemistry of P-glycoprotein-mediated multidrug resistance. Annu. Rev. Biochem. *58*, 137–171.

Fisher, M. H., and Mrozik, H. (1992). The chemistry and pharmacology of avermectins. Annu. Rev. Pharmacol. Toxicol. *32*, 537–553.

Ford, J. M., and Hait, W. N. (1990). Pharmacology of drugs that alter multidrug resistance in cancer. Pharmacol. Rev. *42*, 155–199.

Georges, E., Bradley, G., Gariepy, J., and Ling, V. (1990). Detection of P-glycoprotein isoforms by gene-specific monoclonal antibodies. Proc. Natl. Acad. Sci. USA *87*, 152–156.

Goldstein, G. W., and Betz, A. L. (1986). The blood–brain barrier. Sci. Am. *255*, 70–79.

Goldstein, L. J., Galski, H., Fojo, A., Willingham, M., Lai, S.-L., Gazdar, A., Pirker, R., Green, A., Crist, W., Brodeur, G. M., Lieber, M., Cossman, J., Gottesman, M. M., and Pastan, I. (1989). Expression of a multidrug resistance gene in human cancers. J. Natl. Cancer Inst. *81*, 116–124.

Gottesman, M. M., and Pastan, I. (1993). Biochemistry of multidrug resistance mediated by the multidrug transporter. Annu. Rev. Biochem. *62*, 385–427.

Greig, N. H., Soncrant, T. T., Shetty, H. U., Momma, S., Smith, Q. R., and Rapoport, S. I. (1990). Brain uptake and anticancer activities of vincristine and vinblastine are restricted by their low cerebrovascular permeability and binding to plasma constituents in rat. Cancer Chemother. Pharmacol. *26*, 263–268.

Gros, P., Croop, J., and Housman, D. (1986a). Mammalian multidrug resistance gene: complete cDNA sequence indicates strong homology to bacterial transport proteins. Cell *47*, 371–380.

Gros, P., Ben-Neriah, Y., Croop, J., and Housman, D. E. (1986b). Isolation and expression of a complementary DNA that confers multidrug resistance. Nature *323*, 728–731.

Gros, P., Raymond, M., Bell, J., and Housman, D. (1988). Cloning and characterization of a second member of the mouse *mdr* gene family. Mol. Cell. Biol. *8*, 2770–2778.

Gros, P., Dhir, R., Croop, J., and Talbot, F. (1991). A single amino acid substitution strongly modulates the activity and substrate specificity of the mouse mdr1 and mdr3 drug efflux pumps. Proc. Natl. Acad. Sci. USA *88*, 7289–7293.

Horton, J. K., Thimmaiah, K. N., Houghton, J. A., Horowitz, M. E., and Houghton, P. J. (1989). Modulation by verapamil of vincristine pharmacokinetics and toxicity in mice bearing human tumor xenografts. Biochem. Pharmacol. *38*, 1727–1736.

Hsu, S. I., Lothstein, L., and Horwitz, S. B. (1989). Differential overexpression of three *mdr* gene family members in multidrug-resistant J774.2 mouse cells. J. Biol. Chem. *264*, 12053–12062.

Juliano, R. L., and Ling, V. (1976). A surface glycoprotein modulating drug permeability in Chinese hamster ovary cell mutants. Biochim. Biophys. Acta *455*, 152–162.

Kaster, K. R., Burgett, S. G., Rao, R. N., and Ingolia, T. D. (1983). Analysis of a bacterial hygromycin B resistance gene by transcriptional and translational fusions and by DNA sequencing. Nucl. Acids Res. *11*, 6895–6911.

Laduron, P. M., and Leysen, J. E. (1979). Domperidone, a specific in vitro dopamine antagonist, devoid of in vivo central dopaminergic activity. Biochem. Pharmacol. *28*, 2161–2165.

Levin, V. A. (1980). Relationship of octanol/water partition coefficient and molecular weight to rat brain capillary permeability. J. Med. Chem. *23*, 682–684.

Pulliam, J. D., Seward, R. L., Henry, R. T., and Steinberg, S. A. (1985) Investigating ivermectin toxicity in collies. Vet. Med. *80*, 33–40.

Raymond, M., and Gros, P. (1989). Mammalian multidrug-resistance gene: correlation of exon organization with structural domains and duplication of an ancestral gene. Proc. Natl. Acad. Sci. USA *86*, 6488–6492.

Raymond, M., Rose, E., Housman, D. E., and Gros, P. (1990). Physical mapping, amplification, and overexpression of the mouse *mdr* gene family in multidrug-resistant cells. Mol. Cell. Biol. *10*, 1642–1651.

Roninson, I. B., Chin, J. E., Choi, K., Gros, P., Housman, D. E., Fojo, A., Shen, D.-W., Gottesman, M. M., and Pastan, I. (1986). Isolation of human *mdr* DNA sequences amplified in multidrug-resistant KB carcinoma cells. Proc. Natl. Acad. Sci. USA *83*, 4538–4542.

Saeki, T., Ueda, K., Tanigawara, Y., Hori, R., and Komano, T. (1993). Human P-glycoprotein transports cyclosporin A and FK506. J. Biol. Chem. *268*, 6077–6080.

Sambrook, J., Fritsch, E. F., and Maniatis, T. (1989). Molecular Cloning: A Laboratory Manual, Second Edition (Cold Spring Harbor, New York: Cold Spring Harbor Laboratory Press).

Schinkel, A. H., Roelofs, M. E. M., and Borst, P. (1991). Characterization of the human *MDR3* P-glycoprotein and its recognition by P-glycoprotein-specific monoclonal antibodies. Cancer Res. *51*, 2628–2635.

Sikic, B. I. (1993). Modulation of multidrug resistance: at the threshold. J. Clin. Oncol. *11*, 1629–1635.

Slater, L. M., Sweet, P., Stupecky, M., and Gupta, S. (1986). Cyclosporin A reverses vincristine and daunorubicin resistance in acute lymphatic leukemia in vitro. J. Clin. Invest. *77*, 1405–1408.

Smit, J. J. M., Schinkel, A. H., Oude Elferink, R. P. J., Groen, A. K., Wagenaar, E., van Deemter, L., Mol, C. A. A. M., Ottenhoff, R., van der Lugt, N. M. T., van Roon, M. A., van der Valk, M. A., Offerhaus, G. J. A., Berns, A. J. M., and Borst, P. (1993). Homozygous disruption of the murine *mdr2* P-glycoprotein gene leads to a complete absence of phospholipid from bile and to liver disease. Cell *75*, 451–462.

Sugawara, I., Kataoka, I., Morishita, Y., Hamada, H., Tsuruo, T., Itoyama, S., and Mori, S. (1988). Tissue distribution of P-glycoprotein encoded by a multidrug-resistant gene as revealed by a monoclonal antibody, MRK16. Cancer Res. *48*, 1926–29.

Tanigawara, Y., Okamura, N., Hirai, M., Yasuhara, M., Ueda, K., Kioka, N., Komano T., and Hori, R. (1992). Transport of digoxin by human P-glycoprotein expressed in a porcine kidney epithelial cell line (LLC-PK1). J. Pharm. Exp. Ther. *263*, 840–845.

Tatsuta, T., Naito, M., Oh-hara, T., Sugawara, I., and Tsuruo, T. (1992). Functional involvement of P-glycoprotein in blood–brain barrier. J. Biol. Chem. *267*, 20383–20391.

Taylor, H. G., Pacqué, M., Muñoz, B., and Greene, B. M. (1990). Impact of mass treatment of onchocerciasis on the transmission of infection. Science *250*, 116–118.

Teeter, L. D., Becker, F. F., Chisari, F. V., Li, D., and Kuo, M. T. (1990). Overexpression of the multidrug resistance gene *mdr3* in spontaneous and chemically induced mouse hepatocellular carcinomas. Mol. Cell. Biol. *10*, 5728–5735.

Thiebaut, F., Tsuruo, T., Hamada, H., Gottesman, M. M., Pastan, I., and Willingham, M. C. (1987). Cellular localization of the multidrug resistance gene product in normal human tissues. Proc. Natl. Acad. Sci. USA *84*, 7735–7738.

Thiebaut, F., Tsuruo, T., Hamada, H., Gottesman, M. M., Pastan, I., and Willingham, M. C. (1989). Immunohistochemical localization in normal tissues of different epitopes in the multidrug transport protein P170: evidence for localization in brain capillaries and cross-reactivity of one antibody with a muscle protein. J. Histochem. Cytochem. *37*, 159–164.

Trezise, A. E. O., Romano, P. R., Gill, D. R., Hyde, S. C., Buchwald, M., and Higgins, C. F. (1992). The multidug resistance and cystic fibrosis genes have complementary patterns of epithelial expression. EMBO J. *11*, 4291–4303.

Tsuruo, T., Iida, H., Tsukagoshi, S., and Sakurai, Y. (1981). Overcoming of vincristine resistance in P388 leukemia in vivo and in vitro through enhanced cytotoxicity of vincristine and vinblastine by verapamil. Cancer Res. *41*, 1967–1972.

Ueda, K., Cardarelli, C., Gottesman, M. M., and Pastan, I. (1987). Expression of a full-length cDNA for the human "*mdr1*" gene confers resistance to colchicine, doxorubicin, and vinblastine. Proc. Natl. Acad. Sci. USA *84*, 3004–3008.

Ueda, K., Okamura, N., Hirai, M., Tanigawara, Y., Saeki, T., Kioka, N., Komano, T., and Hori, R. (1992). Human P-glycoprotein transports cortisol, aldosterone, and dexamethasone, but not progesterone. J. Biol. Chem. *267*, 24248–24252.

Valverde, M. A., Diaz, M., Sepúlveda, F. V., Gill, D. R., Hyde, S. C., and Higgins, C. F. (1992). Volume regulated channels associated with the human multidrug-resistance P-glycoprotein. Nature *355*, 830–833.

van der Bliek, A. M., Kooiman, P. M., Schneider, C., and Borst, P. (1988). Sequence of *mdr3* cDNA encoding a human P-glycoprotein. Gene *71*, 401–411.

van der Lugt, N., Robanus Maandag, E., te Riele, H., Laird, P. W., and Berns, A. (1991). A *pgk::hprt* fusion as a selectable marker for targeting of genes in mouse embryonic stem cells: disruption of the T-cell receptor δ-chain-encoding gene. Gene *105*, 263–267.

van Dommelen, F. S., Hamer, C. M., and de Jonge, H. R. (1986). Efficient entrapment of large and small compounds during vesiculation of intestinal microvilli. Biochem. J. *236*, 771–778.

van Tellingen, O., Beijnen, J. H., Nooijen, W. J., and Bult, A. (1993a). Plasma pharmacokinetics of vinblastine and the investigational *Vinca* alkaloid N-(deacetyl-O-4-vinblastoyl-23)-L-ethyl isoleucinate in mice as determined by high-performance liquid chromatography. Cancer Res. *53*, 2061–2065.

van Tellingen, O., Beijnen, J. H., Nooijen, W. J., and Bult, A. (1993b). Tissue disposition, excretion and metabolism of vinblastine in mice as determined by high-performance liquid chromatography. Cancer Chemother. Pharmacol. *32*, 286–292.